Low temperature mixed-mode debond fracture and fatigue characterisation of foam core sandwich

Farshidi, Arash; Berggreen, Christian; Carlsson, Leif A.

Published in:
Journal of Sandwich Structures and Materials

Link to article, DOI:
10.1177/1099636218779420

Publication date:
2020

Document Version
Publisher's PDF, also known as Version of record

JOURNAL OF SANDWICH STRUCTURES & MATERIALS

Original Article

Journal of Sandwich Structures & Materials
2020, Vol. 22(4) 1039–1054

DOI: 10.1177/1099636218779420
journals.sagepub.com/home/jsm
SAGE

Low temperature mixed-mode debond fracture and fatigue characterisation of foam core sandwich

Arash Farshidi[1], **Christian Berggreen**[1] and **Leif A Carlsson**[2]

Abstract

This paper experimentally investigates the effects of low temperature on fracture toughness and fatigue debond growth rate in foam core sandwich composites. Mixed-mode bending specimens were statically and cyclically tested inside a climatic chamber at a low temperature (−20°C) and at room temperature (23°C) as a reference. Testing was conducted in mode I (opening) and mixed-mode I/II (opening-sliding) mode mixities. The fatigue tests results are presented according to the modified Paris–Erdogan relation. Results showed substantial fracture toughness reduction due to low temperature. Low temperature furthermore elevated the cyclic crack growth rate.

Keywords

Mixed-mode bending, low temperature, sandwich, face/core interface, fracture toughness, fatigue crack propagation

[1]Department of Mechanical Engineering, Technical University of Denmark, Kongens Lyngby, Denmark
[2]Department of Ocean and Mechanical Engineering, Florida Atlantic University, Boca Raton, USA

Corresponding author:
Christian Berggreen, Technical University of Denmark, Nils Koppels Alle, Building 404, Kongens Lyngby 2800, Denmark.
Email: cbe@mek.dtu.dk

Introduction

Sandwich composite materials are being used more and more in a wide range of industries. Experience has shown that a serious problem for sandwich composite structures is the existence of debonds at the face/core interface. Such a failure mode compromises the load-carrying capacity of the sandwich structure. The assessment of the criticality of debond damage in sandwich structures is crucial for the further expansion of sandwich structure applications. Many methods and approaches have been proposed by researchers to characterise debond fracture. The mixed-mode bending (MMB) test method is capable of characterising the fracture toughness of delaminations in composite laminates over a wide range of mode I/II mode mixities [1]. This test has recently been extended to face/core interface fracture characterisation of sandwich specimens by Quispitupa et al. [2]. Analytical expressions derived for the compliance and energy release rate for the sandwich MMB specimen showed good agreement with finite element analysis. Manca et al. [3] examined crack growth in debonded MMB foam core sandwich specimens under both quasi-static and cyclic loading. The face/core interface fracture toughness and fatigue crack growth rate of E-glass/polyester and H45 and H100 polyvinyl chloride (PVC) foam core specimens were determined. Later G-controlled cyclic interface crack propagation tests were performed on similar sandwich MMB specimens with a range of foam cores by Manca et al. [4]. The results reveal that the interface crack propagated more rapidly when the foam core density decreased and the mode mixity was changed towards pure mode I.

Arctic operations are becoming increasingly important for naval vessels due to global warming and the need to regularly patrol cold regions. Damage tolerance assessment of vessels operating in such regions is therefore important. For sandwich structures, this includes the characterisation of low temperature debond growth. Gupta and Shukla [5] studied the blast performance of foam core sandwich composites at -40 and 22°C. The main failure mechanisms observed at -40°C were face/core debonding and core cracking. They observed brittle cracking in the M100 foam core specimens at -40°C. The investigation of low-velocity impact response of PVC foam core sandwich composites highlighted the effect of debonding on the post-impact compression strength of sandwich structures [6,7]. The effects of low temperature, seawater and impact on the performance of sandwich composites loaded in four-point bending were studied by Singh and Davidson [8]. The results at 20 and -20°C showed that reducing the temperature for dry undamaged specimens had no effect on their stiffness. Siriruk et al. [9] tested single cantilever beam H100 foam core sandwich specimens inside a climatic chamber. Their results showed that the combined effect of sea water and low temperature (-10°C) substantially reduced the face/core interface fracture toughness. They also found that low temperatures did not significantly affect the elastic modulus, E, for dry specimens. Ural et al. [10] measured the face/core fracture toughness of honeycomb sandwich panels at 24 and -54°C using a double cantilever beam (DCB) test. The results showed a drop of 19–25% in the fracture toughness at the lower temperature. However, to the best

knowledge of the authors, no comprehensive investigation has yet been reported on the effect of low temperature on mixed-mode fracture and fatigue of foam core sandwich specimens.

This current paper reports an experimental study of low temperature mixed-mode debond fracture in sandwich composite specimens with H100 PVC foam core and E-glass/epoxy face sheets, using the a MMB test set-up inside a climatic chamber. MMB specimens were tested at two mode mixity phase angles (mode I and mixed mode) at low temperature (−20°C) and at room temperature (RT) (23°C). Quasi-static and G-controlled fatigue tests were carried out to characterise debond fracture toughness and debond growth rate, respectively.

Experimental procedure

Specimens and test set-up

Sandwich panels consisting of E-glass/epoxy face laminates and a H100 PVC foam core were prepared using vacuum-assisted resin transfer moulding. The face sheets consisted of four DBLT-850-E10 quadri-axial mats with a fibre orientation of $(0/45/90/-45)_s$ which provides quasi-isotropic behaviour in the plane of the laminate. The epoxy resin was RIM135/RIMH137. Both faces were injected simultaneously and the resin provided bonding to the foam core. The nominal thickness of the face laminates was 2 mm. The mode mixity (to be discussed) depends on core thickness and lever position. Core thicknesses were 10 and 20 mm. Lever positions, c, were 65 and 20 mm (see Figure 1).

The mechanical properties of the face sheets and core are listed in Table 1. All specimens were in a rectangular beam shape with 215 mm length, 35 mm width, span length of 160 mm (2L) and face sheet thickness of 2 mm (see Figure 1).

A common method to prepare an artificial face/core debond is to insert a Teflon film between face and core prior to the manufacturing process [3,4]. Unfortunately, this method results in the formation of a resin-rich zone at the end of the Teflon sheet. The resin-rich zone often proves to be tougher than the core, and as a result fracture may occur in the core just beneath the resin-rich zone [12]. Pre-cracking may circumvent this problem, but the crack may kink into the face [4]. Therefore, an artificial crack was machined in the core at a small distance below the face/core interface using a thin bandsaw. As the artificial crack is located inside the foam core, there is no resin-rich zone at the crack tip. The bandsaw procedure, however, did not lead to a sharp crack tip, thus the first propagation increment of the crack for all specimens was considered as pre-cracking and the corresponding data were disregarded. Typically, the pre-cracking increment included the first 2–3 mm crack propagation of all specimens tested.

In order to conduct low temperature testing at temperatures typical for the Arctic region, an Instron EC1637 & AH1637 micro climatic chamber was used. The climatic chamber consists of two main units, a chamber surrounding the test fixture and an air handler unit connected to a liquid nitrogen tank and supplying

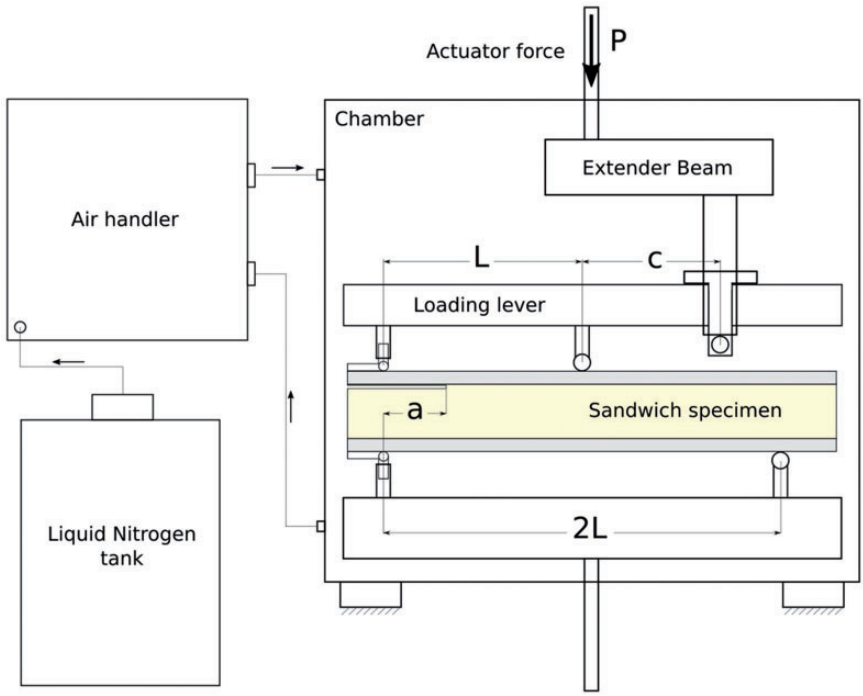

Figure 1. Schematic test set-up and climatic chamber supplied with liquid nitrogen.

Table 1. Mechanical properties of E-glass face sheets and H100 PVC foam core [4, 11].

Properties	value
Face sheet: DBLT-850 $(0/45/90/-45)_s$	
Young's modulus (E_1) (GPa)	18.6
Young's modulus (E_2) (GPa)	18.0
Young's modulus (E_3) (GPa)	9.5
Poisson's ratio (ν_{12})	0.40
Poisson's ratio (ν_{13})	0.37
Poisson's ratio (ν_{23})	0.43
Shear modulus (G_{12}) (GPa)	6.1
Shear modulus (G_{13}) (GPa)	2.7
Shear modulus (G_{23}) (GPa)	2.8
Foam core: H100 PVC	
Cell size (mm)	0.45
Density (kg/m^3)	100
Compressive modulus (MPa)	135
Shear modulus (MPa)	35
Coefficient of thermal expansion (10^{-6}/°C)	40

PVC: polyvinyl chloride.

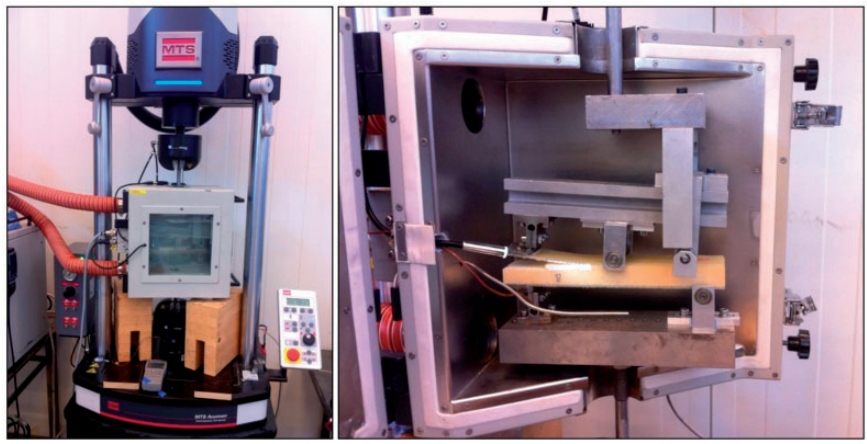

Figure 2. Sandwich MMB test set-up inside a climatic chamber.

cold air through hoses to the chamber (see Figure 1). The test temperature inside the chamber was monitored and controlled. An additional thermometer was used to measure the effective temperature at the surface of the specimen core. In order to ensure a uniform temperature inside the specimen, thermal equilibrium time was measured for one specimen and adopted with a margin for all the specimens. All low temperature specimens were kept at the test temperature for 90 min prior to testing and after the surface temperature had reached the intended value.

All tests were performed in a 3 kN MTS Acumen electrodynamic test machine with a 3 kN load cell mounted and controlled by an MTS FlexTest 40 digital controller. The MTS TestSuite software package was utilised to carry out the quasi-static and fatigue tests.

Figure 2 shows the actual MMB test set-up with a specimen inside the climatic chamber mounted in the test machine. The MMB test fixture was chosen due to its ability to apply mixed-mode loading and keep the mode mixity constant while the crack propagates. The MMB test fixture was modified in order to be able to operate inside the small climate chamber. To allow testing at different lever arm distances c, an extender beam was adopted (see Figure 1). Full-field digital image correlation measurements of displacement of the entire MMB specimen and the test fixture were performed in order to ensure the validity of the displacement measurements taken from the piston movement of the test machine actuator. It was confirmed that the extender beam transfers the applied displacement properly and the modified test set-up provides adequate test conditions.

MMB formulation

The MMB test fixture and specimen are outlined in Figure 1. It has been shown that the sandwich MMB specimen can be considered as a superposition of the

cracked sandwich beam (CSB) mode II specimen and the DCB mode I specimen [2]. The MMB compliance and energy release rate depend on the specimen geometry, loading configuration and mechanical properties of the specimen. Analytical expressions for the MMB specimen compliance, C, and energy release rate, G, have been derived previously [2]

$$C = \left[\frac{c}{L}C_{DCB\_upper} + \frac{c-L}{2L}C_{DCB\_lower}\right]\left(\frac{c}{L} - \alpha\frac{c+L}{2L}\right) + \left(\frac{c+L}{L}\right)^2 C_{CSB} \tag{1}$$

$$\begin{aligned} G = {} & \frac{P^2}{2b^2}\left(\frac{c}{L}\left(\frac{c}{L} - \alpha\frac{c+L}{2L}\right)\frac{12}{E_f h_f^3}\left[a^2 + 2a\eta^{\frac{1}{4}} + \eta^{\frac{1}{2}}\right]\right) \\ & + \frac{P^2}{2b^2}\left(\frac{c-L}{2L}\left(\frac{c}{L} - \alpha\frac{c+L}{2L}\right)\left[\frac{1}{h_c G_{xz}} + \frac{a^2}{D - \frac{B^2}{A}}\right]\right. \\ & \left. + \left(\frac{c+L}{L}\right)^2\left(\frac{a^2}{8}\left[\frac{1}{D_{debonded}} - \frac{1}{D_{intact}}\right]\right)\right) \end{aligned} \tag{2}$$

where P is the applied load; b is the width of specimen; c is the lever arm distance; L is the span length between the supports; α is a load partitioning factor [2]; E_f is the face elastic modulus; h_f and h_c are face and core thickness, respectively; a is the crack length; η is elastic foundation modulus parameter [2]; G_{xz} is the core shear modulus; A, B and D are the extensional, coupling and bending stiffnesses; $D_{debonded}$ and D_{intact} are the flexural stiffnesses of the debonded region and intact region of the cracked beam; and C_{DCB_upper}, C_{DCB_lower} and C_{CSB} are compliance terms of the upper DCB part (i.e. upper face in the debonded region), lower DCB part (i.e. core and lower face in the debonded region) and CSB, respectively. Further details are provided in Quispitupa et al. [2].

The mode mixity phase angle is a measure of the ratio between the relative mode II sliding and mode I opening displacements, δ_x and δ_y of the crack flanks

$$\psi_R = \tan^{-1}\left(\frac{\delta_x}{\delta_y}\right) \tag{3}$$

The phase angle was calculated using the crack surface displacement extrapolation method [13] implemented in a 2D plane strain finite element analysis. The face sheets and foam core were modelled as isotropic with RT mechanical properties (see Table 1). The mode mixity at the crack tip is controlled by the lever arm position, c (Figure 1). Small values of c lead to mixed-mode loading at the crack tip and larger c values provide more dominance of mode I. Mode I dominant

Table 2. Test matrix. Each test condition employed two replicate test specimens.

Test condition	Static	Fatigue	Mode I ($\psi_R = 4.4°$)	Mode II ($\psi_R = -23.9°$)	−20°C	23°C
LTSI	x		x		x	
RTSI	x		x			x
LTSII	x			x	x	
RTSII	x			x		x
LTFI		x	x		x	
RTFI		x	x			x
LTFII		x		x	x	
RTFII		x		x		x

LT: low temperature; RT: room temperature; S: static; F: fatigue.

($\psi_R = 4.4°$) and mixed mode with a significant mode II contribution ($\psi_R = -23.9°$) conditions were selected.

Fracture toughness characterisation

Static fracture testing was conducted at −20 and 23°C. A total of eight specimens were loaded in displacement control with 0.5 mm/min rate inside the climatic chamber to determine the crack propagation load, P_c, as guided by the MMB test standard for monolithic composites [14]. P_c is defined as the maximum load, or the load at which the compliance has increased by 5%, depending on which occurs first along the load–displacement curve. Substituting the measured P_c in equation (2) leads to the critical energy release rate (i.e. the fracture toughness), G_c. At both temperatures, tests were carried out at two c values (i.e. 65 and 20 mm) to obtain the intended mode mixity phase angle, ψ_R. Table 2 is the test matrix where LT and RT represent low and room temperature, S and F are static and fatigue test and I and II indicate mode I and mode II.

Fatigue testing

Fatigue debond growth characterisation was carried out using the G-control test methodology [15], which allows controlled fatigue crack growth testing using real-time control of the cyclic energy release rate (ΔG) at a constant level. This is achieved by automatically controlling the maximum and minimum applied displacements on the fly during the fatigue test [15]. The G-control method monitors compliance based on the measured load and displacement at user-defined time intervals defined by a given number (n) of cycles. By back calculating the corresponding crack length, a, from the compliance, ΔG can be determined by substituting the maximum and minimum loads and a into equation (2). The measured value of ΔG is compared with the desired value, and if needed the maximum and minimum displacements are adjusted by small increments to maintain both constant

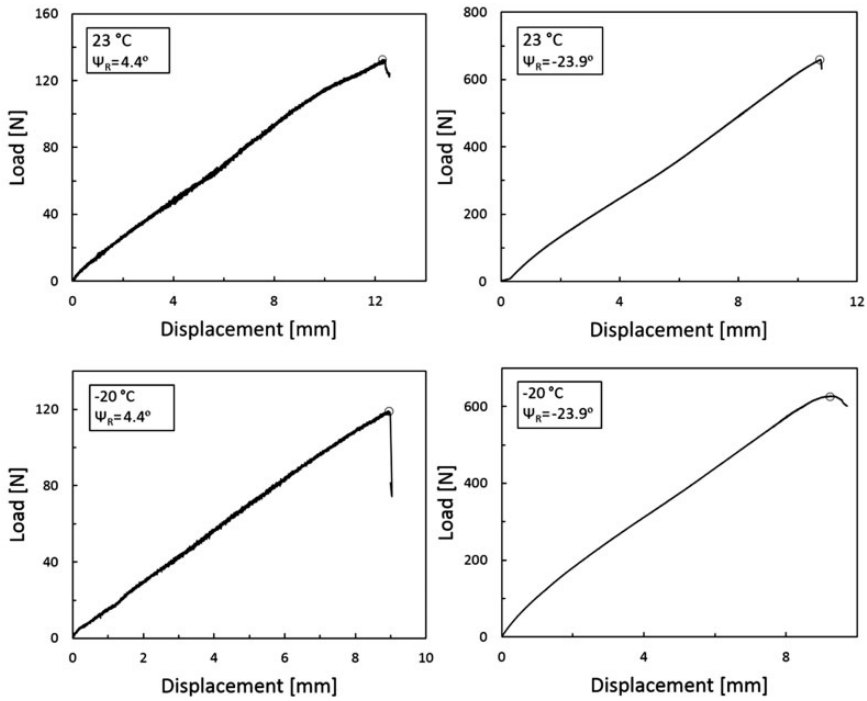

Figure 3. Experimental load versus displacement curves for four different test cases.

ΔG and constant R ratio, and n more cycles are subsequently run. For further details, refer to Manca et al. [15].

Fatigue tests were carried out on eight MMB specimens at a constant testing frequency of 1 Hz and a load ratio of $R = P_{min}/P_{max} = \delta_{min}/\delta_{max} = 0.1$ over a ΔG range of 190–530 J/m^2 using the MTS TestSuite digital controller software. Fatigue tests were performed at two mode mixities and two temperatures in the same way as the static tests (i.e. two replicate specimens for each testing conditions) (see Table 2).

Results and discussion

Fracture toughness

Figure 3 shows examples of experimental load versus displacement measurements at two temperatures and two phase angles. The critical propagation load is marked by an open circle on the curve.

For most specimens the crack growth was stable and the test was stopped after a crack growth increment of 3–5 mm. Multiple fracture tests were therefore conducted on the same specimen. Critical crack propagation load, P_c, at different

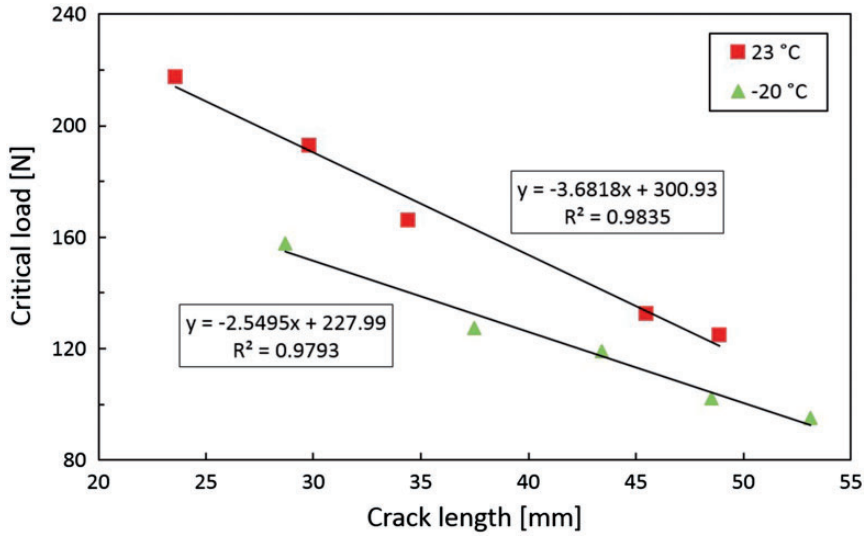

Figure 4. Critical load versus crack length at $\psi_R = 4.4°$

crack lengths was measured both at RT and at −20°C for two different mode mixities (see Figures 4 and 5). At any given crack length, a, significant reduction of the critical load is observed when the temperature is reduced to −20°C.

Compliance was determined for all test cases at both test temperatures (see Figures 6 and 7). The curves are least-squares fits to the experimental data. These results show that a temperature change in this range has no substantial effect on the compliance of the specimen, confirming earlier observations [8].

Fracture toughness, G_c, was determined from equation (2) based on critical loads measured over a range of crack lengths (see Figures 4 and 5). The results (not shown) revealed an almost constant G_c, independent of crack length for each test. Figure 8 shows the average values of fracture toughness for the two mode mixities at room (23°C) and low (−20°C) temperatures. As found by previous researchers [3,16], mode I-dominated loading leads to less fracture toughness than mixed-mode loading. For both phase angles it is noted that reduced temperature leads to reduction of the fracture toughness. The fracture toughness reduction is also influenced by the mode mixity. For $\psi_R = -23.9°$ the reduction is 12%, while for $\psi_R = 4.4°$, the reduction is 32%.

The temperature decrease coupled with different coefficients of thermal expansion (CTE) of the face and core materials in the sandwich composite leads to thermally induced stresses in face sheets and core. These stresses will partially release upon crack propagation and may thus contribute to the crack propagation force. In order to determine the thermally induced energy release rate, an analysis was conducted using the commercial finite element software, ABAQUS [17]. A MMB specimen subject to a temperature decrease (i.e. 23 to −20°C) with no

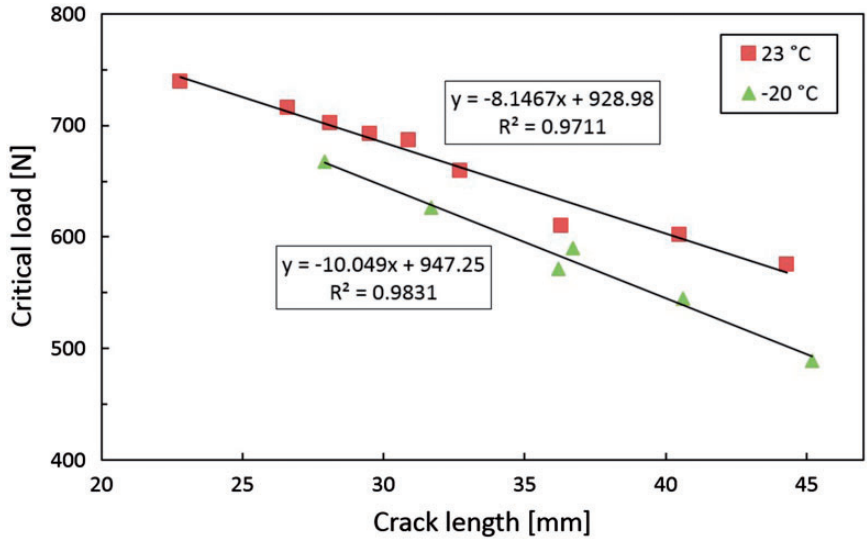

Figure 5. Critical load versus crack length at $\psi_R = -23.9°$

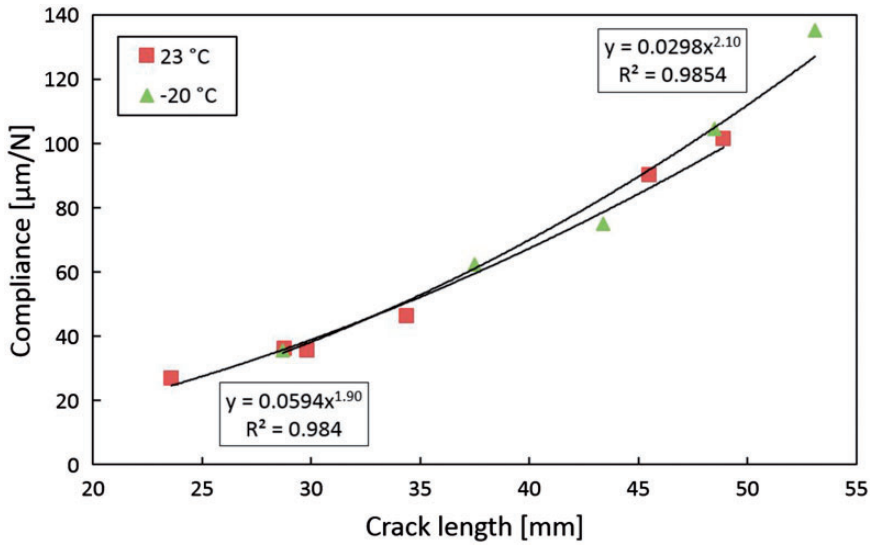

Figure 6. Compliance versus crack length at $\psi_R = 4.4°$ (c=65 mm).

external mechanical loading was modelled using 20-node quadratic brick element (C3D20R). The minimum element size was 0.01 mm and 8340 elements were used. Longitudinal and transverse CTEs of a unidirectional E-glass/epoxy ply were taken from Karadeniz and Kumlutas [18]. The effective CTE of the

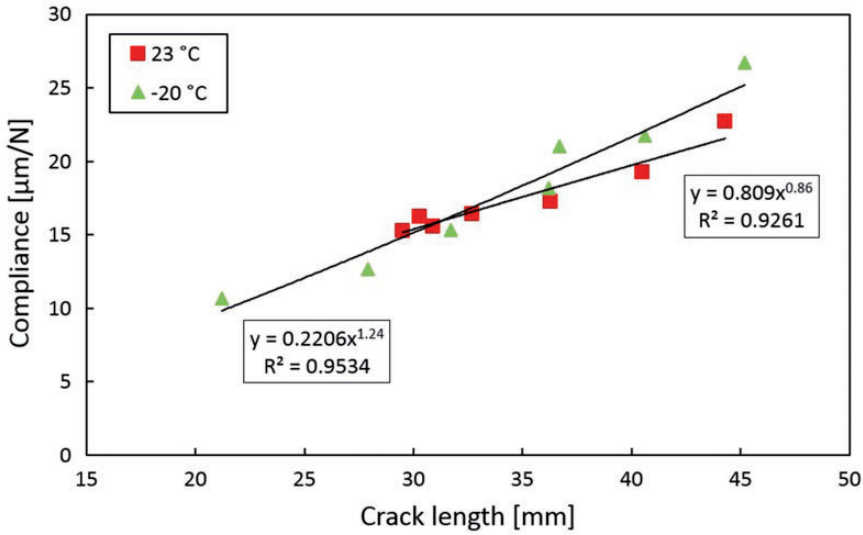

Figure 7. Compliance versus crack length at $\psi_R = -23.9^\circ$ (c=20 mm).

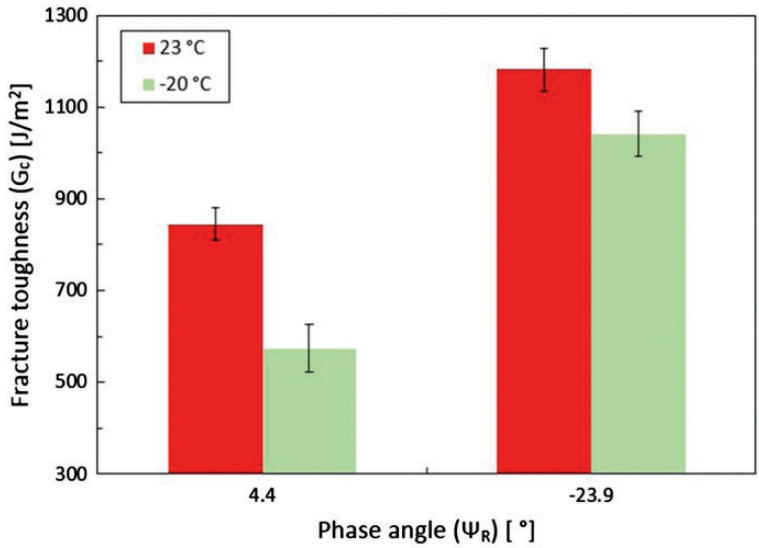

Figure 8. Fracture toughness versus mode mixity phase angle.

quasi-isotropic face laminate was then calculated using classical lamination theory, $15.3 \times 10^{-6}/^\circ$C. CTE of the core is $40 \times 10^{-6}/^\circ$C [11]. The thermally induced energy release rate was calculated using the J-integral in ABAQUS; $G = 1.97$ J/m^2. In order to check the sensitivity of the analysis result to the input parameters (i.e.

Table 3. Effect of variation in the face sheets and core material properties on the energy release rate.

	Face sheet				Core			
	E = 18.6 (GPa)		CTE = 15.3 (10^{-6}/°C)		E = 135 (MPa)		CTE = 40 (10^{-6}/°C)	
	+20%	−20%	+20%	−20%	+20%	−20%	+20%	−20%
Thermally induced G (J/m^2)	1.974	1.969	1.517	2.492	2.364	1.579	3.459	0.903

CTE: coefficients of thermal expansion.

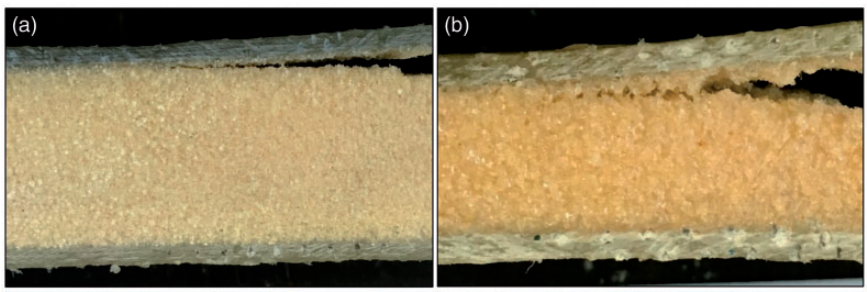

Figure 9. Debond path for specimens tested at −20°C. (a) Mode I-dominated loading conditions and (b) mixed-mode loading conditions.

Young's modulus and CTE of core and face sheets), a sensitivity analysis was carried out for a ±20% change in the Young's modulus and CTEs of the face and core (see Table 3). This analysis provided an energy release rate in the range from 0.90 to 3.46 J/m^2. The maximum of G value is below 0.5% of the measured fracture toughness. Hence, the thermally induced energy release may be neglected.

Fatigue test results

For the G-controlled fatigue propagation tests, the crack propagation path was recorded in each specimen by taking photos of the edge during and after the test. The crack propagated below the resin-rich layer at the face/core interface for all specimens, regardless of mode mixity and temperature. Figure 9 shows crack paths for specimens tested at −20°C. Debond growth took place close to the interface in the mode I-dominated specimens (Figure 9(a)) and presented a smoother crack surface than for the mixed-mode specimens (Figure 9(b)). The mixed-mode specimens tested at −20°C showed smoother crack surfaces than those tested at RT (results are not shown). For mode I-dominated tests, the crack surfaces' roughness was similar at both temperatures. No kinking into the face sheet or fibre bridging was observed.

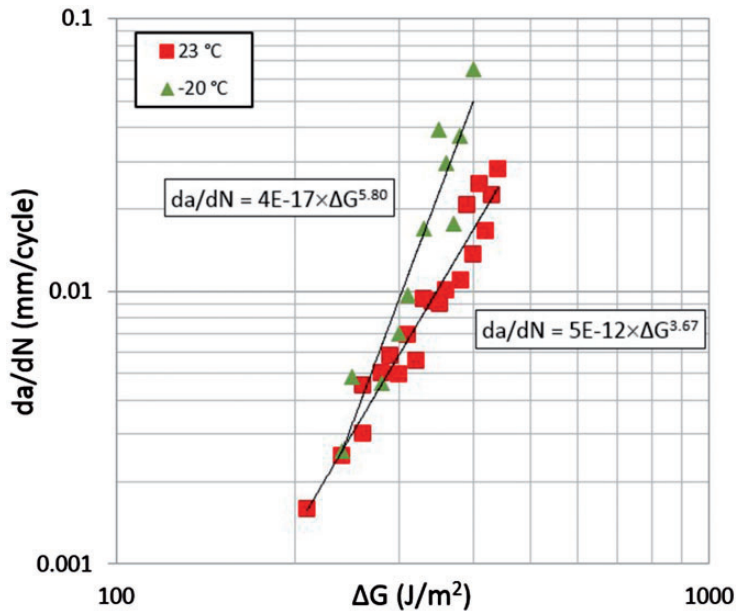

Figure 10. *da/dN* versus ΔG results at $\psi_R = 4.4°$.

The fatigue crack growth test results are shown in Figures 10 and 11 in the form of *da*/*dN* versus ΔG diagrams. Each point represents a test carried out for an increment of crack propagation of 3–4 mm at a constant ΔG. A modified Paris–Erdogan relation [19], equation (4), is used to characterise the crack growth rate

$$\frac{da}{dN} = C_1(\Delta G)^m \tag{4}$$

The results in Figures 10 and 11 show that the crack growth rate depends on both temperature and mode mixity. For mode I conditions ($\psi_R = 4.4°$), a temperature reduction from 23 to −20°C resulted in a slight increase in crack growth rate (see Figure 10). It is noted that the growth results display more scatter at a phase angle $\psi_R = -23.9°$ (Figure 11). More importantly, for $\psi_R = -23.9°$, a reduction of the temperature from 23 to −20°C resulted in a significant increase of crack growth speed. The characteristic parameters C_1 and m in equation (4) were determined by least square curve fitting. The values of the power law exponents, m, are provided in the graphs (Figures 10 and 11). For the RT mode I- and mode II-dominated tests, $m = 3.7$ and 1.3. These values are similar to the RT results reported in Manca et al. [4] and Saenz et al. [20]. Further investigation on the effect of the material properties on the change of fracture toughness and crack growth speed at low temperature can be conducted.

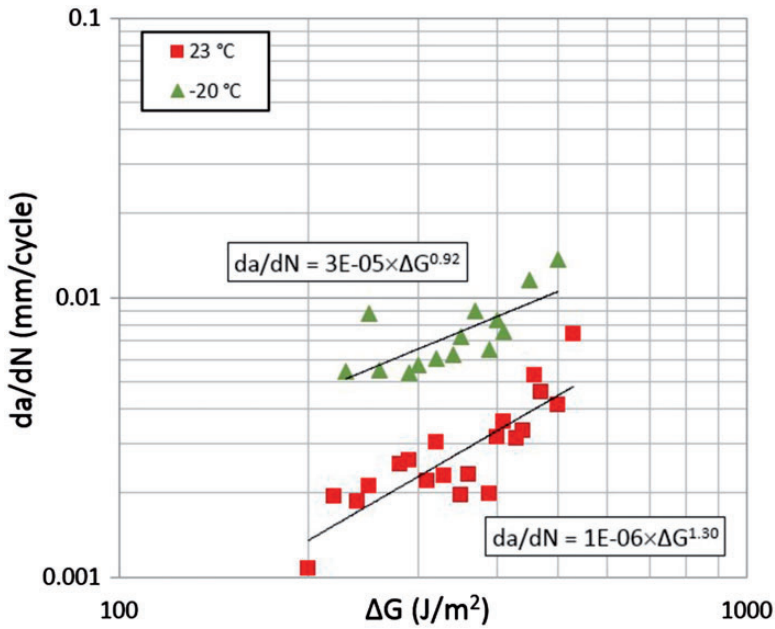

Figure 11. *da/dN* versus ΔG results at $\psi_R = -23.9°$.

Conclusions

Mixed-mode face/core fracture toughness characterisation of foam core sandwich specimens was carried out at 23 and −20°C. At both temperatures the toughness was much less at mode I-dominated conditions than under mixed-mode conditions. It was found that the fracture toughness decreased as the temperature was reduced. The fracture toughness reduction was greater for mode I-dominated loading condition than for mixed-mode loading condition. It was also shown that the stiffness properties of the foam core sandwich composite remained almost unchanged, independent of the temperature. In cyclic debond propagation testing reduced temperature led to increased crack propagation speed. The increase of the crack propagation speed due to temperature decrease was substantially higher for mixed-mode loading than for mode I-dominated loading. The thermally induced energy release rate was also found to be negligible.

Acknowledgements

The support, interest and encouragement of the grant monitor, Dr Y.D.S. Rajapakse, are gratefully acknowledged. We thank Dr Marcello Manca for assistance with G-control test methodology and fatigue testing.

Declaration of Conflicting Interests

The author(s) declared no potential conflicts of interest with respect to the research, authorship, and/or publication of this article.

Funding

The author(s) disclosed receipt of the following financial support for the research, authorship, and/or publication of this article: The work was supported by the Office of Naval Research, Grant N00014-14-1-0253.

ORCID iD

Arash Farshidi http://orcid.org/0000-0002-8286-0914

References

1. Reeder JR and Crews JR. Mixed-mode bending method for delamination testing. *AIAA J* 1990; 28: 420–441.
2. Quispitupa A, Berggreen C and Carlsson LA. On the analysis of a mixed mode bending sandwich specimen for debond fracture characterization. *Eng Fract Mech* 2009; 76: 594–613.
3. Manca M, Quispitupa A, Berggreen C, et al. Face/core debond fatigue crack growth characterization using the sandwich mixed mode bending specimen. *Compos Part A* 2012; 43: 2120–2127.
4. Manca M, Beggreen C, Carlsson LA, et al. Fatigue characterization of poly vinyl chloride (PVC) foam core sandwich composite using the G-control method. *J Sandw Struct Mater* 2016; 18: 374–394.
5. Gupta S and Shukla A. Blast performance of marine foam core sandwich composites at extreme temperatures. *Exp Mech* 2012; 52: 1521–1534.
6. Ozdemir O, Karakuzu R and AL-Shamary AKJ. Core-thickness effect on the impact response of sandwich composites with poly(vinyl chloride) and poly(ethylene terephthalate) foam cores. *J Compos Mater* 2015; 49: 1315–1329.
7. Al-Shamary AKJ, Karakuzu R and Ozdemir O. Low-velocity impact response of sandwich composites with different foam core configurations. *J Sandw Struct Mater* 2016; 18: 754–768.
8. Singh AK and Davidson BD. Effects of temperature, seawater and impact on the strength, stiffness, and life of sandwich composites. *J Reinf Plast Compos* 2010; 30: 269–277.
9. Siriruk A, Penumadu D and Sharma A. Effects of seawater and low temperatures on polymeric foam core material. *Exp Mech* 2012; 52: 25–36.
10. Ural A, Zehnder AT and Ingraffea AR. Fracture mechanics approach to facesheet delamination in honeycomb: measurement of energy release rate of the adhesive bond. *Eng Fract Mech* 2003; 70: 93–103.
11. DIAB. *Technical manual, Divinycell H*. Laholm, 2016, http://www.diabgroup.com
12. Quispitupa A, Berggreen C and Carlsson LA. Face/core interface characterization of mixed mode bending sandwich specimens. *Fatigue Fract Eng Mater Struct* 2011; 34: 839–853.

13. Berggreen C, Simonsen B and Borum K. Experimental and numerical study of interface crack propagation in foam cored sandwich beams. *J Compos Mater* 2007; 41: 493–520.
14. A. D6671/D6671M-13. *Standard test method for mixed mode I-mode II interlaminar fracture toughness of unidirectional fiber reinforced polymer matrix composites*. West Conshohocken, PA: American Society for Testing and Materials, 2013.
15. Manca M, Berggreen C and Carlsson LA. G-control fatigue testing for cyclic crack propagation in composite structures. *Eng Fract Mech* 2015; 149: 375–386.
16. Krueger R. Virtual crack closure technique: history, approach, and applications. *Appl Mech Rev* 2004; 57: 109–143.
17. *Abaqus/Standard® 6.14-2*. Providence, RI, USA: Dassault Systemes Simulia Corporation.
18. Karadeniz HZ and Kumlutas D. A numerical study on the coefficient of thermal expansion of fiber reinforced composite materials. *Compos Struct* 2007; 78: 1–12.
19. Paris P and Erdogan F. A critical analysis of crack propagation laws. *J Basic Eng* 1963; 85: 528–534.
20. Saenz EE, Carlsson LA, Salivar GC, et al. Fatigue crack propagation in polyvinylchloride and polyethersulfone polymer foams. *J Sandw Struct Mater* 2014; 16: 42–65.